Phonon-assisted transport through suspended carbon nanotube quantum dots

Tie-Feng Fang,[1,2] Qing-feng Sun,[2] and Hong-Gang Luo[1,3]

[1]*Center for Interdisciplinary Studies and Key Laboratory for Magnetism & Magnetic Materials of the Ministry of Education, Lanzhou University, Lanzhou 730000, China*

[2]*Institute of Physics, Chinese Academy of Sciences, Beijing 100080, China*

[3]*Beijing Computation Science Research Center, Beijing 100080, China*

(Received 14 August 2011; revised manuscript received 24 September 2011; published 13 October 2011)

Motivated by several recent experiments, we investigate phonon-assisted electronic transport through suspended carbon nanotube quantum dots including electron-electron, electron-phonon, and spin-orbit interactions. By effectively decoupling the electron and phonon thermodynamics, we present an explanation for the puzzling thermoinduced vibrational absorption sidebands, as well further predict that these absorption sidebands are obviously diminished in the partially filled Coulomb diamonds due to the destructive superposition of electron and hole states. The spin-orbit coupling is shown to split all phonon-assisted sidebands while the Kramers degeneracy remains. Interestingly, in the strong spin-orbit coupling regime, some split absorption sidebands are suppressed by the Coulomb blockade effect, while all split emission sidebands always survive.

DOI: 10.1103/PhysRevB.84.155417 PACS number(s): 73.63.−b, 71.38.−k, 71.70.Ej, 73.23.Hk

I. INTRODUCTION

Quantum dots (QDs) formed within suspended carbon nanotubes (CNTs) are promising nanoelectromechanical systems[1] due to their exceptional electronic and mechanical properties. Such QD systems are characterized by a remarkably strong electromechanical coupling.[2–4] Their transport spectroscopy has revealed generic vibrational sidebands[4–7] which arise from electronic tunneling processes mediated by emission or absorption of phonons. These phonon-assisted processes can become the dominant mechanism in the polaronic transport through systems with strong electron-phonon (EP) coupling.[8,9] Indeed, the recent experiment[4] on high-quality CNT samples is able to access this transport regime, allowing the observation of exotic features of the vibrational sidebands, such as the fourfold periodicity, the Franck-Condon blockade, the shift of Coulomb diamond tips, and even the surprising appearance of absorption sidebands for increasing temperatures. The last observation is unexpected since thermally induced absorption sidebands are theoretically shown to be impossible.[9] The underlying physics has not yet been understood.[4]

It is also well established that in ultraclean CNT QDs the confined electrons are subject to an enhanced spin-orbit (SO) coupling due to the tube curvature.[10,11] Remarkably, energy scales of the measured SO interaction range from a few 100 μeV to a few meV,[10,11] being comparable with characteristic scales (i.e., phonon energies) of the observed vibrational sidebands, at least for the longitudinal stretching mode of CNTs.[4,5] Interesting physics then arises when the two scales merge in the same systems. By studying such cases, insights into the influence of the SO coupling on the polaronic transport through suspended CNT QDs can be brought.

In this paper we address these issues within a model taking account of electron-electron (EE), EP, and SO interactions for suspended CNT QDs. We combine the nonequilibrium Keldysh technique,[12] polaronic transformation,[13,14] and equation of motion (EOM) approach[12,15] to demonstrate the polaronic transport properties of the system. These, for negligible SO coupling, concur well with the experiment.[4] In particular, based on an EP nonequilibrium thermodynamics, the thermally induced absorption sidebands are reproduced, and are further shown to be more prominent in the empty and fully filled Coulomb diamonds than in partially filled ones where phonon-absorbed tunnelings are taking place through mixed electron and hole states. For strong SO coupling, phonon-assisted tunnelings manifest as vibrational sidebands splitting in the Kramers sector. The conductance characteristics are thus heavily modified. In this regime, the Coulomb blockade effect plays an important role in determining the intensities of split absorption sidebands.

The rest of the paper is organized as follows. In Sec. II, we introduce the relevant model Hamiltonian and solve the transport problem for suspended CNT QDs. Numerical results and their discussions are presented in Sec. III. Finally, Sec. IV is devoted to a summary.

II. THEORY

Suspended CNTs support several quantized vibrational modes which, for a small dot formed within the long suspended segment, only couple to the intradot charge with different Holstein coupling strength.[7,16] The dominantly coupled mode is the longitudinal stretching mode[16] whose phonon energy ε_p is inversely proportional to the CNT length.[5] On the other hand, the electronic states of CNT QDs form four-electron shell structures, representing twofold spin and orbital degrees of freedom. In the lowest shell, the four SO states were thought to be degenerate. Inclusion of SO interaction then splits this fourfold degeneracy into two Kramers doublets.[17,18] As a result, the low-energy electronic spectrum of CNT QDs can be written as[19] $\varepsilon_{\sigma\lambda} = \varepsilon_d - \sigma\lambda\Delta/2$. Here ε_d is the bare level which can be tuned by a gate voltage; $\sigma,\lambda = \pm$ are quantum numbers labeling two spin and orbital states, respectively; and Δ is the strength of SO coupling which is inversely proportional to the CNT diameter.[10,18] Restricting ourselves

to the filling of one shell, we model a suspended CNT QD coupled to source (L) and drain (R) leads by the following Anderson-Holstein Hamiltonian

$$\mathcal{H} = \sum_m \varepsilon_m \hat{d}_m^\dagger \hat{d}_m + \frac{U}{2} \sum_{m\neq m'} \hat{n}_m \hat{n}_{m'} + M\hat{n}(\hat{b}^\dagger + \hat{b}) + \varepsilon_p \hat{b}^\dagger \hat{b} + \sum_{k,m,\alpha} [\varepsilon_k \hat{c}_{km\alpha}^\dagger \hat{c}_{km\alpha} + (V_\alpha \hat{c}_{km\alpha}^\dagger \hat{d}_m + \text{H.c.})], \quad (1)$$

where the index $m \equiv \{\sigma,\lambda\}$ is a combination of the spin and orbital indices, labeling the four SO states, $\hat{d}_m^\dagger$ ($\hat{c}_{km\alpha}^\dagger$) creates an electron of energy ε_m (ε_k) in the dot [α lead ($\alpha = L,R$)], $\hat{n} = \sum_m \hat{n}_m$ with $\hat{n}_m = \hat{d}_m^\dagger \hat{d}_m$ means the total dot charge, U denotes the on-site EE Coulomb repulsion, the vibrational mode of the CNT is excited by the phonon operator $\hat{b}^\dagger$, and M is the Holstein EP coupling strength. The dot-lead tunneling is accounted for by the tunnel matrix element V_α which induces an intrinsic linewidth of the dot levels $\Gamma = \sum_\alpha \Gamma_\alpha$ with $\Gamma_\alpha = \pi\rho|V_\alpha|^2$, where ρ is the electronic density of states (EDOS) in the leads.

Within the Keldysh formalism,[12] the electronic current through our system in the wide-band limit is given by $I = \frac{4e}{h}\frac{\pi\Gamma_L\Gamma_R}{\Gamma_L+\Gamma_R}\int d\varepsilon [f_L(\varepsilon) - f_R(\varepsilon)]\rho_d(\varepsilon)$, where $\rho_d(\varepsilon) = -\frac{1}{\pi}\sum_m \text{Im}\, G_m^r(\varepsilon)$ is the local EDOS on the dot, $G_m^r(\varepsilon) = -\frac{i}{\hbar}\int dt\, e^{i\varepsilon t/\hbar}\theta(t)\langle\{\hat{d}_m(t),\hat{d}_m^\dagger\}\rangle_{\mathcal{H}}$ is the dot retarded Green's function (GF) of the Hamiltonian (1) with $\theta(t)$ being the Heaviside step function, and $f_\alpha(\varepsilon)$ represents the Fermi distribution function in the α lead.

In order to elucidate the polaronic transport scenario from this current expression, one needs to solve the dot GF $G_m^r(\varepsilon)$, which includes full correlation effects from the EE, EP, and SO interactions. To this end, we first apply a polaronic transformation[13,14] $\mathcal{H} \to \widetilde{\mathcal{H}} = e^S \mathcal{H} e^{-S}$, with $S = (M/\varepsilon_p)\hat{n}(\hat{b}^\dagger - \hat{b})$, to the Hamiltonian (1). This gives us $\widetilde{\mathcal{H}} = \widetilde{\mathcal{H}}_p + \widetilde{\mathcal{H}}_e$, where $\widetilde{\mathcal{H}}_p = \varepsilon_p \hat{b}^\dagger \hat{b}$ and

$$\widetilde{\mathcal{H}}_e = \sum_m \widetilde{\varepsilon}_m \hat{d}_m^\dagger \hat{d}_m + \sum_{k,m,\alpha} \varepsilon_k \hat{c}_{km\alpha}^\dagger \hat{c}_{km\alpha} + \frac{\widetilde{U}}{2}\sum_{m\neq m'} \hat{n}_m \hat{n}_{m'} + \sum_{k,m,\alpha} (\widetilde{V}_\alpha \hat{c}_{km\alpha}^\dagger \hat{d}_m + \text{H.c.}), \quad (2)$$

with $\widetilde{\varepsilon}_m = \widetilde{\varepsilon}_d - \sigma\lambda\Delta/2$, $\widetilde{\varepsilon}_d = \varepsilon_d - g\varepsilon_p$, $\widetilde{U} = U - 2g\varepsilon_p$, $\widetilde{V}_\alpha = V_\alpha \hat{X}$, and $\hat{X} = \exp[\sqrt{g}(\hat{b} - \hat{b}^\dagger)]$. Here $g = M^2/\varepsilon_p^2$ is a dimensionless measure of EP coupling. Next, we decouple the electronic ($\widetilde{\mathcal{H}}_e$) and phononic ($\widetilde{\mathcal{H}}_p$) dynamics by replacing here the operator $\hat{X}$ with its expectation value $\langle\hat{X}\rangle$. This approximation has been widely used in the literature[20] and is valid for the strong EP interaction $M > \Gamma$ that favors the formation of local polarons,[14,21] as is the case with the experiment.[4] The only effect of $\langle\hat{X}\rangle$ is that it narrows the width of tunneling resonances when the EP coupling is significantly strong. In particular, $\langle\hat{X}\rangle$ and the dot-lead coupling V_α emerge in the form $V_\alpha\langle\hat{X}\rangle$ always. We can thus incorporate the expectation value $\langle\hat{X}\rangle$ into the dot-lead coupling and redefine the renormalized resonance width[22] as $\widetilde{\Gamma}_\alpha = \pi\rho|\widetilde{V}_\alpha|^2$. Evaluating the phonon part of the trace by Feynman disentangling technique,[14] and employing the Keldysh equations for relevant lesser and greater GFs[12] that collect all electron and hole contributions,[23] the desired dot GF $G_m^r(\varepsilon)$ can then be expressed in this polaronic representation

$$\text{Im}\, G_m^r(\varepsilon) = \sum_{n=-\infty}^{\infty} L_n \big\{ f(\varepsilon + n\varepsilon_p)\text{Im}\, \widetilde{G}_m^r(\varepsilon + n\varepsilon_p) + [1 - f(\varepsilon - n\varepsilon_p)]\text{Im}\, \widetilde{G}_m^r(\varepsilon - n\varepsilon_p)\big\}, \quad (3)$$

where $\widetilde{G}_m^r(\varepsilon)$ is the dot retarded GF with respect to the Hamiltonian $\widetilde{\mathcal{H}}_e$, $n \in \mathbb{Z}$, $f(\varepsilon) = \sum_\alpha \widetilde{\Gamma}_\alpha f_\alpha(\varepsilon)/\widetilde{\Gamma}$, and $L_n = \exp\{-g[1 + 2N(\varepsilon_p)]\}\{[N(\varepsilon_p) + 1]/N(\varepsilon_p)\}^{n/2} I_n(x)$ with $x = 2g\sqrt{N(\varepsilon_p)[N(\varepsilon_p) + 1]}$. Here we have introduced the modified Bessel function of the first kind $I_n(x)$ and the Bose distribution function $N(\varepsilon_p)$. L_n is actually the Franck-Condon factor which characterizes the envelope of vibrational sidebands. At zero temperature, it reduces to $L_n = e^{-g} g^n/n!$ for $n \geqslant 0$, otherwise $L_n = 0$. We emphasize that the phonon (T_p) and electron (T_e) temperatures[24] respectively entering $N(\varepsilon_p)$ and $f_\alpha(\varepsilon)$ can be different, since for such EP-coupled systems, a global thermal equilibrium between the electrons in the bulk leads and local phonons in the dot region can usually not be reached when a current is present.[24]

To calculate the dot GF $\widetilde{G}_m^r(\varepsilon)$, we employ the EOM approach[12,15] generalized to involve the fourfold electronic states in CNT QDs with the SO coupling. Here the EOM takes into account all relevant tunneling processes and can be applied straightforwardly for the electron subsystem $\widetilde{\mathcal{H}}_e$ already decoupled from the phonon one. We finally obtain the dot GF as[12,15]

$$\widetilde{G}_m^r(\varepsilon) = \prod_{j=1}^4 P_{jm}^{-1}(\varepsilon)\Bigg[\prod_{j=2}^4 P_{jm}(\varepsilon) + \widetilde{U}\prod_{j=3}^4 P_{jm}(\varepsilon)\sum_{m'}{}' n_{m'} + \widetilde{U}^2 P_{4m}(\varepsilon)\sum_{m',m''}{}' n_{m'}n_{m''} + \widetilde{U}^3 \sum_{\substack{m',m'',\\ m'''}}{}' n_{m'}n_{m''}n_{m'''}\Bigg], \quad (4)$$

where the primes above three summations mean $m' \neq m, m' \neq m'' \neq m$, and $m' \neq m'' \neq m''' \neq m$, respectively, $P_{jm}(\varepsilon) = \varepsilon - \widetilde{\varepsilon}_m - (j-1)\widetilde{U} + i\widetilde{\Gamma}$, and $n_m = \langle\hat{n}_m\rangle_{\widetilde{\mathcal{H}}_e} = -\frac{1}{\pi}\int d\varepsilon\, f(\varepsilon)\,\text{Im}\, \widetilde{G}_m^r(\varepsilon)$. $\widetilde{G}_m^r(\varepsilon)$ can thus be self-consistently calculated.

III. RESULTS AND DISCUSSIONS

In the numerical results presented below, we fix $\widetilde{U} = 5\varepsilon_p = 40\widetilde{\Gamma} = 0.1D$ with the lead half bandwidth $D = 1$, and apply a symmetric source-drain bias voltage V. The dot levels $\widetilde{\varepsilon}_m$ are measured from the equilibrium Fermi level $\mu = 0$, which lies at the middle of the band. In typical experiments, the dot level and hence the electron occupancy on the dot are tuned by an applied gate voltage. We thus introduce a renormalized gate voltage $V_g \equiv 1/2 - \widetilde{\varepsilon}_d/\widetilde{U}$ to mimic the number of electrons in the considered shell, i.e., a continuous tuning of the electron occupancy from 0 to 4 is achieved through continuously varying V_g from 0 to 4.

When the SO coupling is negligible, the electronic states of the CNT QD are fourfold degenerate. Consecutive filling of these states by tuning the gate voltage yields the fourfold periodicity of Coulomb diamonds and vibrational

sidebands in the low-temperature conductance map, as shown in Fig. 1. In this figure, the edge lines of the Coulomb diamonds are zero-phonon bands corresponding to electronic tunnelings without invoking phonons, and the lines parallel to the edges are vibrational emission sidebands arising from tunneling processes mediated by emission of phonons. While multiple-phonon processes are exponentially suppressed for weak EP coupling [Fig. 1(a)], they become dominant in the strong-coupling regime where the conductance at low bias is Franck-Condon blockaded [Fig. 1(b)]. Further asymmetrically tuning the dot-lead couplings can suppress the conductance lines with positive (or negative) slope, leading to a shift of the Coulomb diamond tips between positive and negative bias [Fig. 1(c)]. These features agree well with the experiment[4] and are well understood. Additionally, V_g-independent steps at $V = \pm n\varepsilon_p$ are also exhibited in Figs. 1(a)–1(c). These steps, generated by phonon-emitted off-resonant tunnelings due to the QD level broadening, have not been observed in the experiment[4] because they are already smeared out, even at the experimental base temperature $T_0 \sim 0.1\varepsilon_p$ [Fig. 1(d)].

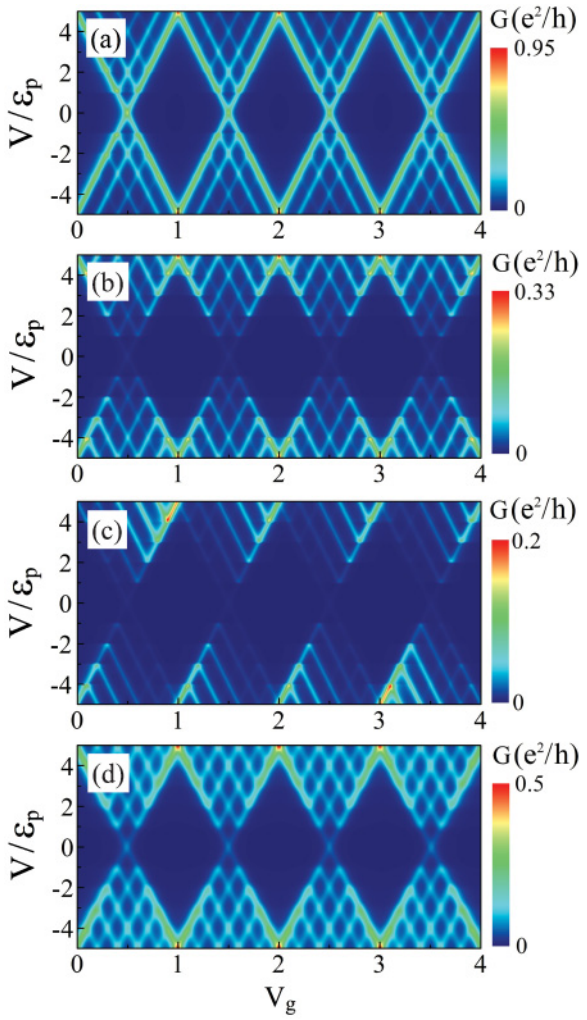

FIG. 1. (Color online) Differential conductance $G \equiv dI/dV$ vs gate voltage V_g and source-drain bias V. (a) $g = 1$, $T_{p(e)} = 0$, $\widetilde{\Gamma}_L = \widetilde{\Gamma}_R$; (b) $g = 5$, $T_{p(e)} = 0$, $\widetilde{\Gamma}_L = \widetilde{\Gamma}_R$; (c) $g = 5$, $T_{p(e)} = 0$, $\widetilde{\Gamma}_L = 0.1\widetilde{\Gamma}_R$; (d) $g = 3$, $T_{p(e)} = 0.1\varepsilon_p$, $\widetilde{\Gamma}_L = \widetilde{\Gamma}_R$.

The most striking and not understood observation of the experiment[4] is the appearance of vibrational absorption sidebands within the Coulomb diamonds as the experimental cryostat temperature is increased. This feature is absent in previous theoretical simulations[9] assuming thermal equilibrium between electrons and phonons. However, such an equilibrium may actually be broken due to (i) the fact that the phonon subsystem is easier to warm up since it has a relatively small heat capacity at low temperature and (ii) the nonequilibrium phonon generation by electronic transport.[25] The negative differential conductance observed in the experiment[4] may also suggest the presence of current-excited phonons with even higher energy[26] which can decay into the relevant stretching mode due to anharmonic effects.[27] For these reasons, a phonon temperature T_p higher than the electron temperature T_e is expected during the heating process of the device. Granted these, our theory reproduces the experimental thermal evolution of the conductance map, with evident absorption sidebands developed in the diamonds before the electron temperature completely smears out all the features [Figs. 2(a)–2(c)]. These sidebands result from phonon-absorbed tunnelings which take place because thermal phonons are available at an elevated phonon temperature. Unlike the emission sidebands, the

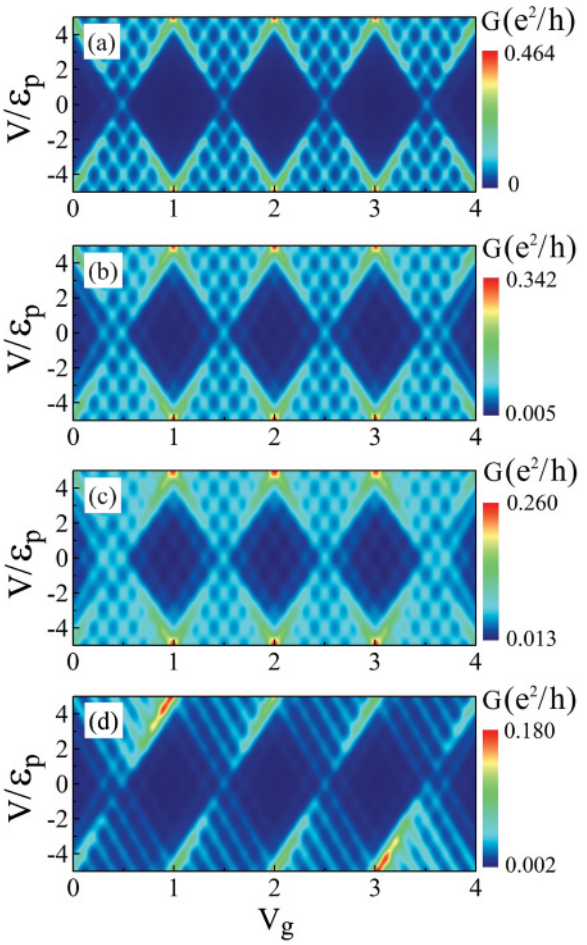

FIG. 2. (Color online) (a)–(c) Thermal evolution of conductance map, $T_{p(e)}/\varepsilon_p = 0.35(0.11)$ (a), 0.7(0.15) (b), and 1.0(0.19) (c), for $\widetilde{\Gamma}_L = \widetilde{\Gamma}_R$. (d) Conductance map at $T_{p(e)}/\varepsilon_p = 0.7(0.15)$ for $\widetilde{\Gamma}_L = 0.1\widetilde{\Gamma}_R$. The EP coupling is fixed at $g = 3$.

absorption ones of positive and negative slopes, corresponding to a given electronic state, are due to the same tunneling processes. They thus have the same intensity even for strongly asymmetric dot-lead couplings [Fig. 2(d)]. Our results here are also consistent with the experimental argument.[4]

More interestingly, while all the Coulomb diamonds demonstrate identical emission sidebands, the absorption sidebands inside the empty ($\langle\hat{n}\rangle = 0$) and fully filled ($\langle\hat{n}\rangle = 4$) diamonds are higher in intensity than those inside the partially filled ($\langle\hat{n}\rangle = 1$–$3$) ones [see Figs. 2(a)–2(d)]. This phenomenon is related to the destructive superposition of electron and hole states, which will become apparent by investigating the local EDOS $\rho_d(\varepsilon)$. Figures 3(a)–3(c) present thermal evolutions of this quantity for three V_g values representative of the empty, partially filled, and fully filled diamonds, respectively. In the local EDOS, the zero-phonon bands lie at $\varepsilon = \widetilde{\varepsilon}_m + (j-1)\widetilde{U}$, $j = 1$–4, representing electron or hole states if they are below or above the Fermi level. These bands produce vibrational sidebands through phonon-emitted or phonon absorbed processes. For electron (hole) states, the absorption and emission sidebands are respectively on the

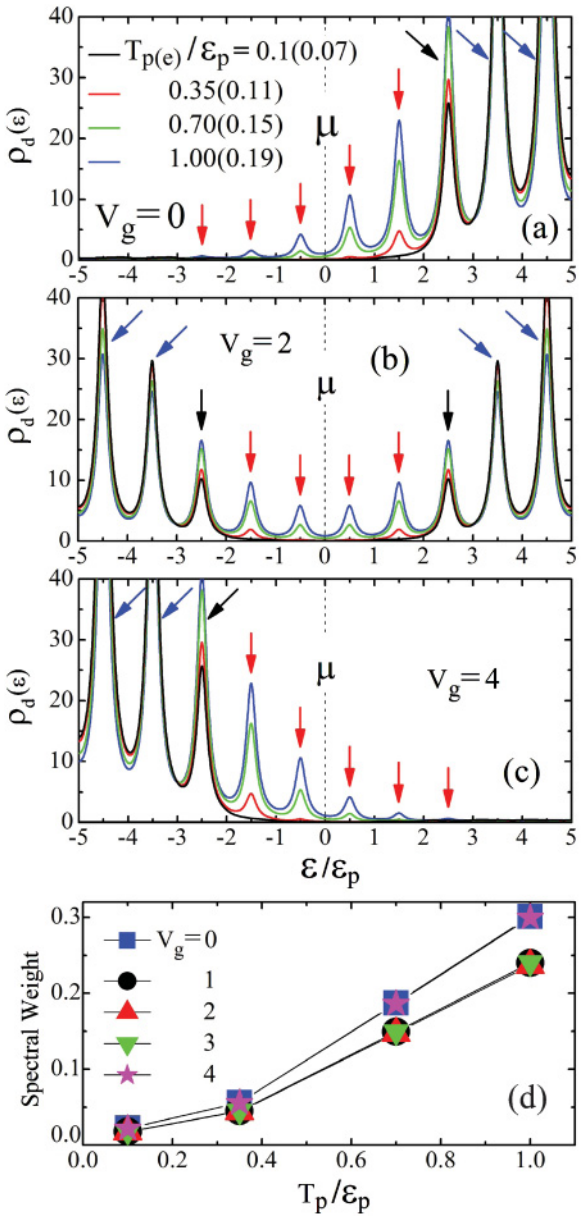

FIG. 3. (Color online) (a)–(c) Thermal evolution of the dot EDOS for different V_g. The black, blue (dark gray), and red (lighter gray) arrows indicate zero-phonon band, emission, and absorption sidebands, respectively. (d) Spectral weight of absorption sidebands in $\rho_d(\varepsilon)$ as a function of T_p. The EP coupling is fixed at $g = 3$ and $\widetilde{\Gamma}_L = \widetilde{\Gamma}_R$ is used throughout.

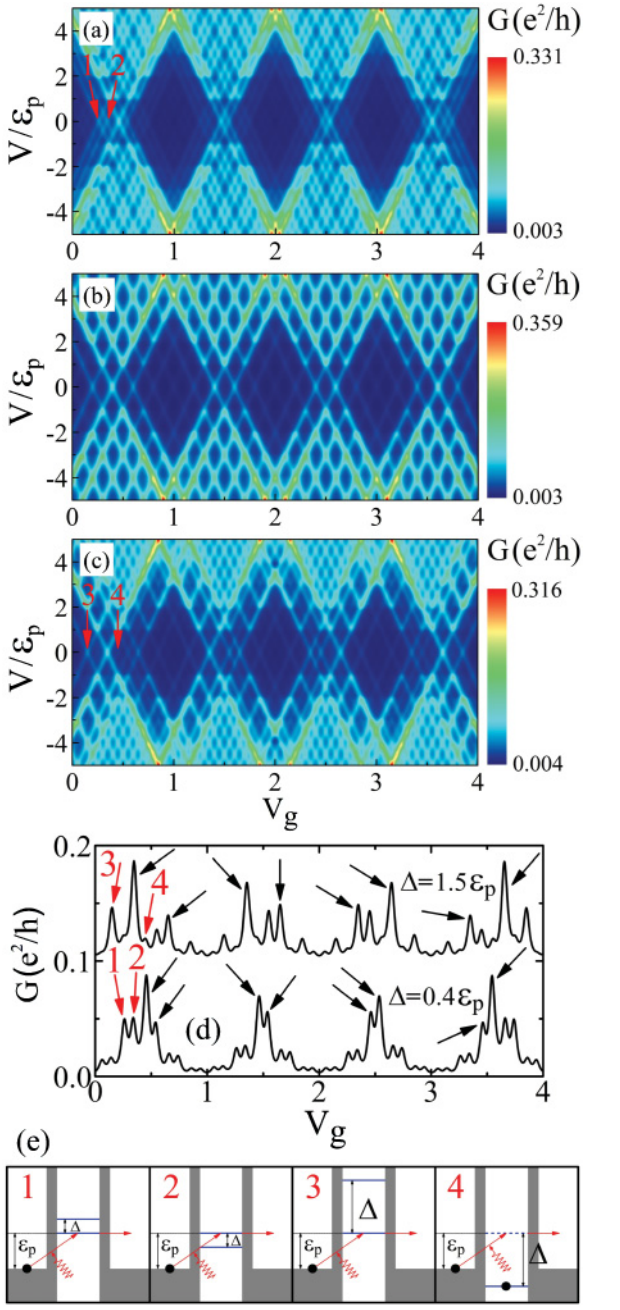

FIG. 4. (Color online) Conductance map for $g = 3$, $T_{p(e)}/\varepsilon_p = 0.6(0.05)$, and $\widetilde{\Gamma}_L = \widetilde{\Gamma}_R$, with SO coupling $\Delta/\varepsilon_p = 0.4$ (a), 1.0 (b), and 1.5 (c). (d) Two lines cut at $V = 0$ in (a) and (c), respectively. The black arrows denote the zero-phonon bands. (e) Schematic diagrams of relevant tunneling processes for absorption sidebands marked by 1, 2, 3, and 4 in (d).

high- (low-) and low- (high-) energy side of the zero-phonon bands. For phonon-assisted transport through the CNT QD under not so large source-drain biases, only the local EDOS near the Fermi level is relevant. In this regime, the absorption sidebands in Figs. 3(a)–3(c) can be respectively attributed to phonon-absorbed hole states, mixed electron-hole states, and electron states, while the emission sidebands are always through phonon-emitted pure electron or hole states. The mixture of electrons and holes for absorption sidebands in the partially filled case [e.g., Fig. 3(b)] is actually a destructive superposition since it significantly reduces the spectral weight as compared with the empty and fully filled cases [Fig. 3(d)]. Considering further the equivalence between electron and hole transport, the different (equivalent) intensities of absorption (emission) sidebands for different diamonds in the maps Figs. 2(a)–2(d) are thus understandable.

For small-diameter CNTs, the SO coupling Δ is rather strong and its interplay with vibrational effect can then be addressed. In this regime, the phonon-assisted tunnelings can take place through two split Kramers doublets, thereby manifesting themselves as split vibrational sidebands at $\Delta < \varepsilon_p$ [Fig. 4(a)]. The adjacent split sidebands due to tunnelings through different Kramers doublets are merged when $\Delta = \varepsilon_p$ where the energy difference of such tunnelings is compensated by emission or absorption of a phonon [Fig. 4(b)], and split further for stronger SO coupling $\Delta > \varepsilon_p$ resulting in a much more complicated pattern [Fig. 4(c)]. Remarkably, though two split absorption sidebands have nearly equal intensities for $\Delta < \varepsilon_p$, the Coulomb blockade effect can make them quite different when one of them crosses a zero-phonon band for $\Delta > \varepsilon_p$ [seen explicitly in Fig. 4(d)]. This is because in the latter case the split absorption sidebands are related to two electronic states with significantly different electron populations in the dot. To illustrate this scenario, we trace the Δ evolution of one representative split pair marked by 1, 2, 3, and 4 with relevant tunneling processes shown in Fig. 4(e). The tunneling 4 is strongly suppressed by Coulomb repulsion of the electron already populating the lower Kramers doublet. This explains the lower intensity of sideband 4 as compared with sidebands 1, 2, and 3. Similar analyses are also applicable to other split absorption sidebands. We emphasize finally that this effect is unique to absorption sidebands and absent in emission ones.

IV. CONCLUSION

In summary, we have studied the phonon-assisted transport through suspended CNT QDs. It is shown that the appearance of the thermally induced vibrational absorption sidebands in the experiment[4] is due to the EP nonequilibrium. These absorption sidebands are further predicted to be significantly suppressed in the partially filled Coulomb diamonds. We also take into account the effect of SO coupling for small-diameter CNTs, thereby demonstrating the splitting of all vibrational sidebands and the Coulomb blockade of some absorption sidebands in the strong SO coupling regime. Further experiments are encouraged to check these predictions.

ACKNOWLEDGMENT

This work was financially supported by NSF-China under Grant Nos. 10821403, 10974236, 10874059, and 11004090, and by the China-973 program.

[1] K. L. Ekinci and M. L. Roukes, Rev. Sci. Instrum. **76**, 061101 (2005).
[2] G. A. Steele, A. K. Hüttel, B. Witkamp, M. Poot, H. B. Meerwaldt, L. P. Kouwenhoven, and H. S. J. van der Zant, Science **325**, 1103 (2009).
[3] B. Lassagne, Y. Tarakanov, J. Kinaret, D. Garcia-Sanchez, and A. Bachtold, Science **325**, 1107 (2009).
[4] R. Leturcq, C. Stampfer, K. Inderbitzin, L. Durrer, C. Hierold, E. Mariant, M. G. Schultz, F. von Oppen, and K. Ensslin, Nat. Phys. **5**, 327 (2009).
[5] S. Sapmaz, P. Jarillo-Herrero, Ya. M. Blanter, C. Dekker, and H. S. J. van der Zant, Phys. Rev. Lett. **96**, 026801 (2006).
[6] B. J. LeRoy, S. G. Lemay, J. Kong, and C. Dekker, Nature (London) **432**, 371 (2004); A. K. Hüttel, B. Witkamp, M. Leijnse, M. R. Wegewijs, and H. S. J. van der Zant, Phys. Rev. Lett. **102**, 225501 (2009); L. Siddiqui, A. W. Ghosh, and S. Datta, Phys. Rev. B **76**, 085433 (2007).
[7] F. Cavaliere, E. Mariani, R. Leturcq, C. Stampfer, and M. Sassetti, Phys. Rev. B **81**, 201303(R) (2010).
[8] J. Koch and F. von Oppen, Phys. Rev. Lett. **94**, 206804 (2005).
[9] J. Koch, F. von Oppen, and A. V. Andreev, Phys. Rev. B **74**, 205438 (2006).
[10] F. Kuemmeth, S. Ilani, D. C. Ralph, and P. L. McEuen, Nature (London) **452**, 448 (2008); S. H. Jhang, M. Marganska, Y. Skourski, D. Preusche, B. Witkamp, M. Grifoni, H. van der Zant, J. Wosnitza, and C. Strunk, Phys. Rev. B **82**, 041404(R) (2010).
[11] H. O. H. Churchill, F. Kuemmeth, J. W. Harlow, A. J. Bestwick, E. I. Rashba, K. Flensberg, C. H. Stwertka, T. Taychatanapat, S. K. Watson, and C. M. Marcus, Phys. Rev. Lett. **102**, 166802 (2009).
[12] H. Haug and A.-P. Jauho, *Quantum Kinetics in Transport and Optics of Semiconductors*, 2nd ed. (Springer, Berlin, 2008).
[13] I. G. Lang and Y. A. Firsov, Sov. Phys. JETP **16**, 1301 (1963).
[14] G. D. Mahan, *Many-Particle Physics*, 3rd ed. (Plenum, New York, 2000).
[15] Y. Meir, N. S. Wingreen, and P. A. Lee, Phys. Rev. Lett. **66**, 3048 (1991); A. Groshev, T. Ivanov, and V. Valtchinov, *ibid*. **66**, 1082 (1991).
[16] E. Mariani and F. von Oppen, Phys. Rev. B **80**, 155411 (2009).
[17] D. V. Bulaev, B. Trauzettel, and D. Loss, Phys. Rev. B **77**, 235301 (2008).
[18] S. Weiss, E. I. Rashba, F. Kuemmeth, H. O. H. Churchill, and K. Flensberg, Phys. Rev. B **82**, 165427 (2010).
[19] T.-F. Fang, W. Zuo, and H.-G. Luo, Phys. Rev. Lett. **101**, 246805 (2008); M. R. Galpin, F. W. Jayatilaka, D. E. Logan, and F. B.

Anders, Phys. Rev. B **81**, 075437 (2010); D. E. Logan and M. R. Galpin, J. Chem. Phys. **130**, 224503 (2009).

[20]David M.-T. Kuo and Y. C. Chang, Phys. Rev. B **66**, 085311 (2002); U. Lundin and R. H. McKenzie, *ibid.* **66**, 075303 (2002); Y.-S. Liu, H. Chen, X.-H. Fan, and X.-F. Yang, *ibid.* **73**, 115310 (2006); Q.-f. Sun and X. C. Xie, *ibid.* **75**, 155306 (2007); M. Galperin, A. Nitzan, and M. A. Ratner, *ibid.* **76**, 035301 (2007); J. Liu, J. Song, Q.-f. Sun, and X. C. Xie, *ibid.* **79**, 161309(R) (2009); L.-L. Zhou, S.-S. Li, J.-N. Wei, and S.-Q. Wang, *ibid.* **83**, 195303 (2011).

[21]A. C. Hewson and D. M. Newns, J. Phys. C **12**, 1665 (1979); **13**, 4477 (1980).

[22]Under the decoupling, the ratio $\widetilde{V}_\alpha / V_\alpha = \langle \hat{X} \rangle$. However, a few references (see Ref. 21) have shown that in some cases the EP coupling does not narrow the width of tunneling resonances, implying $\widetilde{V}_\alpha / V_\alpha = 1$. In the present paper, we take the renormalized resonance width $\widetilde{\Gamma}_\alpha$ as an input parameter instead of the previous bare one Γ_α, so our numerical results are independent of the exact value of the ratio $\widetilde{V}_\alpha / V_\alpha$, except for a constant factor difference.

[23]M. Galperin, A. Nitzan, and M. A. Ratner, Phys. Rev. B **73**, 045314 (2006); Z.-Z. Chen, R. Lü, and B.-F. Zhu, *ibid.* **71**, 165324 (2005).

[24]Y. Dubi and M. D. Ventra, Rev. Mod. Phys. **83**, 131 (2011).

[25]M. Lazzeri, S. Piscanec, F. Mauri, A. C. Ferrari, and J. Robertson, Phys. Rev. Lett. **95**, 236802 (2005); M. Oron-Carl and R. Krupke, *ibid.* **100**, 127401 (2008); S. Berciaud, M. Y. Han, K. F. Mak, L. E. Brus, P. Kim, and T. F. Heinz, *ibid.* **104**, 227401 (2010).

[26]E. Pop, D. Mann, J. Cao, Q. Wang, K. Goodson, and H. Dai, Phys. Rev. Lett. **95**, 155505 (2005).

[27]G. P. Srivastava, *The Physics of Phonons* (IOP, Bristol, UK, 1990).